

## Strange quark as a probe for new physics in the Higgs sector

---

**Valentina Maria Martina Cairo**<sup>a,1,\*</sup>

<sup>a</sup>*Conseil européen pour la recherche nucléaire - CERN,  
Esplanade des Particules 1, P.O. Box 1211 Geneva 23, Switzerland*

*E-mail:* [valentina.maria.cairo@cern.ch](mailto:valentina.maria.cairo@cern.ch)

One of the most interesting yet-to-be answered questions in Particle Physics is the nature of the Higgs Yukawa couplings and their universality. Key information in our understanding of this question arises from studying the coupling of the Higgs boson to second generation quarks. Some puzzles in the flavor sector and potential additional sources of CP violation could also have their origins in an extended Higgs sector. Rare Higgs decay modes to charm or strange quarks are very challenging or nearly impossible to detect with the current experiments at the Large Hadron Collider, where the large multi-jet backgrounds makes it difficult to study light quark couplings with inclusive  $h \rightarrow q\bar{q}$  decays. Future  $e^+e^-$  machines are thus the perfect avenue to study such phenomena.

This contribution presents the development of a novel algorithm for tagging jets originating from the hadronisation of strange quarks (strange-tagging) and the first application of such a strange-tagger to a direct Higgs to strange ( $h \rightarrow s\bar{s}$ ) analysis. The work is performed with the International Large Detector (ILD) concept at the International Linear Collider (ILC), but it is easily applicable to other Higgs factories. The study includes as well a preliminary investigation of a Compact Ring Imaging Cerenkov system (RICH) capable of maximising strange-tagging performance in future Higgs factory detectors.

*41st International Conference on High Energy physics - ICHEP2022  
6-13 July, 2022  
Bologna, Italy*

---

<sup>1</sup>On behalf of the ILD Concept Group

\*Speaker

## 1. Introduction

In 2012, the ATLAS [1] and CMS [2] collaborations at the Large Hadron Collider (LHC) [3] announced the discovery of a particle compatible with the Higgs Boson and in the last ten years we have studied many of its properties and couplings [4, 5]. The measurements of the couplings of the Higgs Boson with the W and Z vector bosons as well as its Yukawa coupling to the top and bottom quark confirm its compatibility with the Standard Model (SM) Higgs Boson ( $h$ ). The coupling of the Higgs boson to lighter generation fermions is yet to be proven. The ATLAS and CMS collaboration reported the first evidence that the Higgs boson decays into two muons [4, 5], indicating its relation with the second-generation leptons, but the path towards understanding the universality of the Yukawa interactions has just began. Rare Higgs decay modes such as those to charm or strange quarks are very challenging or nearly impossible to detect with the existing experiments due to both the detector capabilities and the overwhelming multi-jet production rate at the LHC which inhibits the study of strange, up, and down quark couplings with inclusive  $h \rightarrow q\bar{q}$  decays, in addition to the dominant  $h \rightarrow b\bar{b}$  decay mode. The work published in Ref. [6] shows instead how Future Higgs factories are ideal to probe the coupling of the Higgs boson to light fermions, in particular to the strange quark, but detectors with specific features for particle identification have to be designed.

## 2. Strange-tagging at future $e^+e^-$ colliders

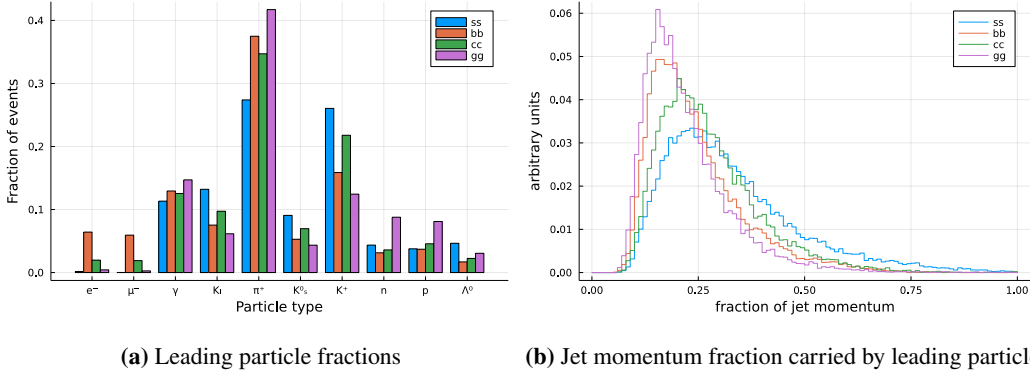


**Figure 1:** (a) Leading particle fractions and (b) the fraction of the jet's momentum carried by the leading particle for reconstructed jets from  $h \rightarrow s\bar{s}/b\bar{b}/c\bar{c}/gg$  events.

Studying the coupling of the Higgs boson to the strange quark relies on the possibility of identifying jets originating from the strange quark hadronisation (strange-tagging), which is a very complex problem. While bottom and charm jets can be differentiated based on the presence of tracks with large impact parameters as well as of 2 or 1 secondary vertices, strange jets, which, excluding  $V^0$ s, have 0 secondary vertices, are only differentiated from light (i.e., up or down) jets based on the presence of a strange hadron within the jet. Strange hadrons are also most often the leading particle in strange jets, as evident from Figure 1a. Furthermore, as shown in Figure 1b, the leading particle carries a larger fraction of the strange jet's momentum as compared to other jet flavours. Therefore, having  $\pi/K$  particle identification (PID) at moderate to high particle momentum (i.e.,  $>10$  GeV), is the key for strange-tagging. To better quantify the impact of PID on strange-tagging, a recurrent

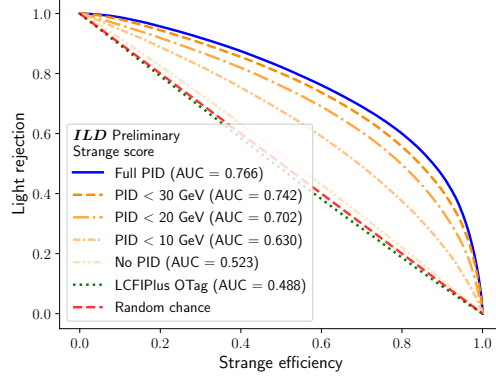


**Figure 2:** Light jet rejection as a function of the strange-tagging efficiency with PID for any particle momentum (“Full PID”), as well as without PID (“No PID”) and with partial PID (“PID <  $X$  GeV”).

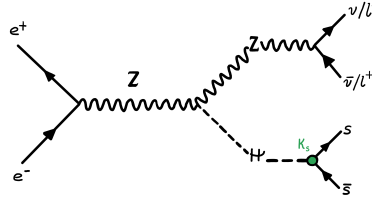
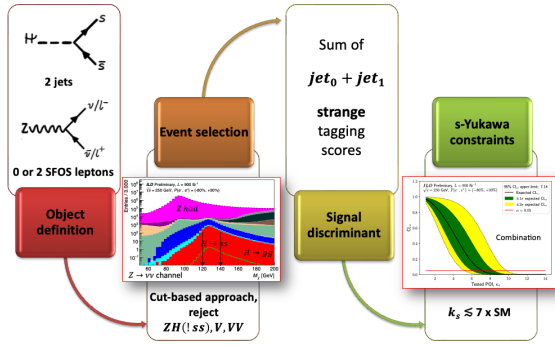
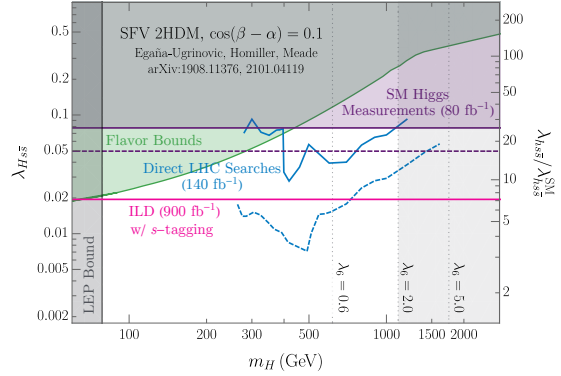
28 Neural Network tagger for classifying jet-flavor was developed. All the details can be found in  
 29 Ref. [6]. It was trained on full simulation  $Z(inv)(h \rightarrow q\bar{q}/h \rightarrow gg)$  samples produced with the  
 30 International Large Detector (ILD) [7, 8] concept at the proposed International Linear Collider [9]<sup>1</sup>.  
 31 The tagger includes per-jet level inputs and kinematic information about the 10 leading particles in  
 32 each jet, including PDG-based likelihoods (for electrons, muons, pions, kaons/strange hadrons and  
 33 protons), to make the study of general validity. Figure 2 shows the light-jet rejection as a function  
 34 of the strange-tagging efficiency in several scenarios: with PID for any particle momentum (“Full  
 35 PID”), as well as for the jet flavour taggers without PID (“No PID”) and with partial PID (“PID  
 36 <  $X$  GeV”). As expected, the performance are poor when no PID is included in the tagger while,  
 37 for example, a 50% strange tagging efficiency with about 80% light-jet rejection is achieved when  
 38 PID is included in the full momentum range. The possibility of having PID at high momentum  
 39 boosts the performance dramatically: as an example, for a fixed 80% rejection, the strange-tagging  
 40 efficiency increases by a factor of 1.5, 2.0 and 2.5 when the momentum range of PID goes up to 10,  
 41 20 or 30 GeV, respectively. A much smaller gain is observed when including PID above 30 GeV.  
 42 This provides clear evidence that to tag strange jets at future colliders,  $\pi/K$  PID capabilities up to  
 43 30 GeV are of paramount importance.

## 44 2.1 $h \rightarrow s\bar{s}$ analysis with the ILD at the ILC

45 It is now of interest to apply the newly developed strange-tagger to a direct search for  $h \rightarrow s\bar{s}$   
 46 with the ILD concept at the ILC. The ILC is foreseen to run at several centre-of-mass energies,  
 47 including a dedicated 250 GeV run for Higgs couplings studies. At such energy, the dominant  
 48 Higgs boson production mechanism is via associated  $Zh$  production, with a cross-section of about  
 49 200 fb. The branching ratio of the SM Higgs boson to strange quark is approximately  $2 \times 10^{-4}$ . As  
 50 a back-of-the-envelope calculation, assuming  $2000 \text{ fb}^{-1}$  of data collected at the ILC after 10 years  
 51 of data-taking and a Higgs boson production cross section of about 200 fb,  $\sim 400,000$  Higgs bosons  
 52 would be produced where only 80 of those feature a  $h \rightarrow s\bar{s}$  event. The Feynman diagram of the  
 53 process can be seen in Figure 3a. As a point of comparison,  $\sim 200,000 h \rightarrow b\bar{b}$  and  $\sim 12,000$

<sup>1</sup>A similar study was performed in the context of the Future Circular Collider and can be found in Ref. [10].

54  $h \rightarrow c\bar{c}$  events are expected. Nevertheless, when considering Beyond the Standard Model (BSM)  
 55 scenarios that allow for extended Higgs sectors, the scenario changes. A particular class of models  
 56 with additional Higgs doublets (2HDM) have new Yukawa matrices which need not be directly  
 57 proportional to the SM fermion masses. One such class of models are those exhibiting spontaneous  
 58 flavour violation (SFV) [11], which allows for new Yukawa couplings either to the up or the down  
 59 quarks with no relation to the quark masses. A two Higgs doublet model with up-type SFV, for  
 60 example, could thus have large couplings to the  $d$  and  $s$  quarks, and the new Higgs states would  
 61 be produced in quark fusion, with decays to gauge and Higgs bosons and quarks [12, 13]. If the  
 62 observed 125 GeV Higgs boson is an admixture of a SM-like Higgs and one of the new Higgs states,  
 63 its couplings to the first or second generation quarks can be significantly larger than predicted in  
 64 the SM, leading to large deviations in the Higgs boson branching ratios.


 (a) Zh with  $h \rightarrow s\bar{s}$  Feynman diagram.

 (b) Flow chart of the Zh with  $h \rightarrow s\bar{s}$  analysis.

 (c)  $CL_s$  upper limit for  $\kappa_s$  in the SFV 2HDM.


**Figure 3:** (a) Tree-level Feynman diagram for production of a Higgs boson in association with a Z boson. The Higgs decays hadronically to strange quarks (with Yukawa coupling strength modifier  $\kappa_s$ ) and the Z decays leptonically to charged leptons or neutrinos. Drawing by F. Cairo. (b) Flow chart of the Zh with  $h \rightarrow s\bar{s}$  analysis. A more detailed description of the analysis flow as well as the figures can be found in Ref. [6]. (c)  $CL_s$  upper limit for  $\kappa_s$  in the context of the SFV 2HDM framework. For more details on its interpretation, see Ref.[6, 12, 13].

65 Figure 3b illustrates schematically the Zh,  $h \rightarrow s\bar{s}$  analysis flow while more detailed informa-  
 66 tion can be found in Ref. [6]. The events are required to have two jets and either 0 or 2 same-flavour  
 67 opposite-sign leptons. Kinematic cuts are then applied to reject the major backgrounds arising from  
 68 single of double vector boson production as well as Zh with the Higgs boson decaying to flavours  
 69 other than the strange. The sum of the leading and sub-leading strange-jet tagging score is used as  
 70 the final signal discriminant to extract the constraints on the strange Yukawa coupling modifier,  $\kappa_s$ ,

71 which is found to be  $k_s \lesssim 7$  when the  $P(e^-, e^+) = (-80\%, +30\%)$  polarisation scenario is used,  
 72 corresponding to  $900 \text{ fb}^{-1}$  of the initial proposed  $2000 \text{ fb}^{-1}$  of data<sup>2</sup>. Figure 3c shows that these  
 73 results, which are still expected to improve with the inclusion of additional polarisation states and  
 74 running scenarios, when interpreted as bounds on the SFV 2HDM model are the strongest through-  
 75 out the parameter space considered, exceeding those expected from measurements performed at the  
 76 High Luminosity LHC (HL-LHC) except for a small range of parameters. Therefore, tests of SFV  
 77 2HDMs are expected to be highly competitive at future lepton colliders like the ILC.

## 78 2.2 Particle Identification

3 $\sigma$ separation for $\pi/K$				
dE/dx in silicon	TOF via Fast Timing in silicon envelopes or calorimetry	dE/dx in Time Projection or Drift Chambers	dN/dx	RICH
$\gtrsim 5 \text{ GeV}$	$\gtrsim 5 \text{ GeV}$	$\gtrsim 30 \text{ GeV}$ (scales with volume)	O(tens of GeV)	O(tens of GeV)



**Figure 4:** Particle identification techniques and the expected momentum range that they cover.

79 When we talk about particle identification for strange-tagging, we are talking about identifying  
 80 hadrons. Hadrons are identified by their mass, in turn determined by combining momentum and  
 81 velocity [14]. Assuming that the momentum is inferred from the radius of curvature in a magnetic  
 82 field, the remaining question is to measure the velocity. There exists several techniques to determine  
 83 velocity, for example Time-of-flight (TOF), ionization losses  $dE/dx$  or cluster counting  $dN/dx$ ,  
 84 transition radiation or Cherenkov radiation. The momentum range covered by these techniques is  
 85 illustrated in Figure 4. ILD has a Time Projection Chamber (TPC) as part of the tracking system,  
 86 which provides PID via measurements of  $dE/dx$ , and it is envisioned to be completed by time-of-  
 87 flight (TOF) measurements in the TPC's silicon envelopes or in the electromagnetic calorimeter.  
 88 This explains the choice of using ILD to study strange-tagging, but from the studies presented in  
 89 Ref. [8], a  $\pi/K$  separation with a  $3\sigma$  significance is reached only up to 20 GeV, as the performance  
 90 scale with the tracker volume. Therefore we have investigated alternative layouts which could  
 91 extend particle identification to higher momentum in future detector concepts.

## 92 2.3 A Compact RICH proposal

93 The Ring Imaging Cherenkov Detector (RICH) is the system that pioneered PID and represents  
 94 a favourable approach at high momentum when using gas as radiators [15]. The important question  
 95 to address is whether it will possible to accommodate a *compact* RICH system while preserving  
 96 performance in tracking and calorimetry at future multi-purpose detectors. Our proposed concept  
 97 to address this question is illustrated in Figure 5a. This Compact RICH detector is designed  
 98 using spherical mirrors and Silicon Photomultipliers (SiPMs) as photon detectors.<sup>3</sup> The layout

<sup>2</sup>In other words, “upper limits” on the upper limits.

<sup>3</sup>The present design with SiPM detectors requires that the total neutron dose at RICH's location is less than  $\sim 5 \times 10^{10} n_{\text{eq}}/10$  years, for which the SiPM damage is expected to be low.

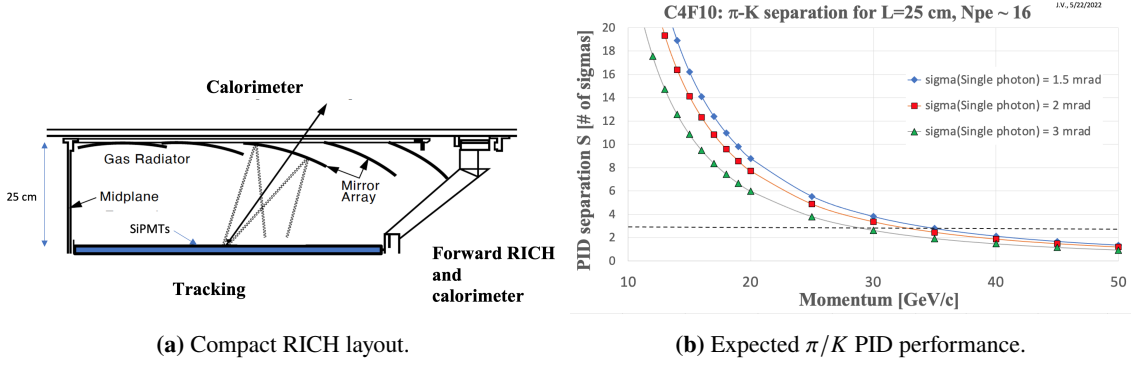


**Figure 5:** (a) Proposed gaseous Compact RICH detector. The relative placement of the tracking, calorimetry, and forward instrumentation is indicated. (b) Expected PID performance as a function of momentum and single-photon Cherenkov angle resolution.

resembles the gaseous RICH detector of the SLAC Large Detector’s (SLD’s) Cherenkov Ring Imaging Detector (CRID) [16]. However, introducing SiPMs improves the PID performance by a factor of two. Furthermore, fast timing SiPMs ( $< 100$  ps) can provide timing information to reject background photons and, at the same time, a TOF system covering the lower momentum range and complementing the RICH. The overall aim is to make this RICH detector with as low mass as possible and its depth as thin as possible because we do not want to degrade the calorimeter. This speaks for mirrors made of beryllium and the structure made of low mass carbon-composite material. Our initial choice of 25 cm in radial depth could be reduced further if the detection efficiency of future photon detectors improve. For example, if the detection efficiency improves by  $\sim 50\%$ , the radial depth can be reduced to 10–15 cm, in turn reducing the magnetic smearing contribution to Cherenkov angle resolution. The study assumes a 5 T magnetic field as a conservative estimate, but Ref. [6] describes the performance also with other magnetic field scenarios, as well as the gas choice and the Cherenkov angle resolution. The estimated performance of the Compact RICH is shown in Figure 5b for a  $C_4F_{10}$  gas as a function of Cherenkov angle resolution. A Cherenkov angle resolution of up to 3 mrad will allow to achieve the desired performance of  $\sigma > 3\sigma$   $\pi/K$  separation up to 30 GeV. Alternative layouts capable of reaching higher momenta include pressurised gas, as presented in Refs. [17, 18]. However, one would need to deal with a vessel holding a pressurised gas and the increase in detector mass becomes significant ( $X/X_0 \sim 10\%$ ), while higher momentum ranges have been proven not to increase strange-tagging drastically. We believe that our design instead can be built with  $X/X_0 \sim 3\text{--}4\%$ . This simple study indicates that modern and compact RICH detectors are a promising solution for PID at future  $e^+e^-$  accelerators and justify full GEANT4 simulations.

### 3. Conclusions

Testing the universality of the Higgs Yukawa coupling is a key benchmark for future Higgs factories. Our ordinary matter is composed by electron and light quarks and none of the Higgs boson couplings to such particles has been verified yet. The Large Hadron Collider as well as its High Luminosity operations will ramp down in about two decades. It is thus a very exciting time to

126 look ahead and think about the design of a future Higgs factory and its detectors, which will allow us  
127 to solve some of the yet-to-be answered questions in Particle Physics. Probing the Strange Yukawa  
128 coupling is both a challenge and an opportunity at Future Colliders, with the interplay between  
129 detector design, performance and analysis techniques being the key to success. Many unexplored  
130 physics benchmarks rely on strange tagging (not only the study of the Higgs boson, but also of Z,W  
131 vector bosons as well as the top quark and flavour physics in general). Strange tagging, in turn, is  
132 enabled by  $\pi/K$  discrimination at high momenta, which can potentially be achieved with a modern  
133 Compact RICH. We demonstrated that stringent constraints can be derived via a direct search for  
134 the SM  $h \rightarrow s\bar{s}$  and the phase space for new physics can be reduced to  $k_s \lesssim 7$  with only  $900 \text{ fb}^{-1}$   
135 of data at an ILC-like future collider.

## 136 References

- 137 [1] The ATLAS Collaboration, <https://www.doi.org/10.1088/1748-0221/3/08/S08003>.
- 138 [2] The CMS Collaboration, <https://www.doi.org/10.1088/1748-0221/3/08/S08004>.
- 139 [3] L. Evans and P. Bryant, <https://www.doi.org/10.1088/1748-0221/3/08/S08001>.
- 140 [4] The ATLAS Collaboration, <https://doi.org/10.1038/s41586-022-04893-w>.
- 141 [5] The CMS Collaboration, <https://doi.org/10.1038/s41586-022-04892-x>.
- 142 [6] A. Albert, M. Basso, S. Bright-Thonney, V. Cairo et al., <https://arxiv.org/abs/2203.07535>.
- 143 [7] T. Behnke et al., <https://arxiv.org/abs/2003.01116>.
- 144 [8] H. Abramowicz et al., <https://arxiv.org/abs/1912.04601>.
- 145 [9] T. Behnke et al., <https://arxiv.org/abs/1306.6327>.
- 146 [10] F. Bedeschi, L. Gouskos, and M. Selvaggi, <https://arxiv.org/abs/2202.03285>.
- 147 [11] D. Egaña-Ugrinovic, S. Homiller, and P. Meade, <https://arxiv.org/abs/1811.00017>.
- 148 [12] D. Egaña-Ugrinovic, S. Homiller, and P. Meade, <https://arxiv.org/abs/1908.11376>.
- 149 [13] D. Egaña-Ugrinovic, S. Homiller, and P. Meade, <https://arxiv.org/abs/2101.04119>.
- 150 [14] R. Forty, <https://indico.cern.ch/event/630418/contributions/2813741>.
- 151 [15] A. Papanestis, <https://doi.org/10.1016/j.nima.2019.03.059>.
- 152 [16] J. Va'vra, [https://doi.org/10.1016/S0168-9002\(99\)00367-8](https://doi.org/10.1016/S0168-9002(99)00367-8).
- 153 [17] R. Forty, <https://indico.cern.ch/event/995850/contributions/4406336>.
- 154 [18] M. Tat, R. Forty, G. Wilkinson, <https://indico.desy.de/event/33640/contributions/128392>.